

## SOIL STRENGTH AND LOAD BEARING CAPACITY MEASUREMENT TECHNIQUES

### Author(s):

A. E. Eltayeb Ahmed<sup>1</sup>, A. El Hariri<sup>1</sup>, P. Kiss<sup>2</sup>

### Affiliation:

<sup>1</sup> Mechanical Engineering Doctoral School – Hungarian University of Agriculture and Life Sciences, 2100 Gödöllő, Páter Károly u. 1., Hungary;

<sup>2</sup> Institute of Technology - Hungarian University of Agriculture and Life Sciences, 2100 Gödöllő, Páter Károly u. 1., Hungary;

### Email address:

Ahmed.Ahmed.Elawad.Eltayeb@phd.uni-mate.hu; El.hariri.alaa.2@phd.uni-mate.hu; Kiss.peter@uni-mate.hu

**Abstract:** In this research, the interest will be given to studying the load bearing capacity and strength of soil terrain, resulting from machine-soil interaction. A small introduction will define terramechanics studies and its importance when dealing with machine-terrain interaction. The axial load acting on a terrain will lead to the sinkage of the machine, thus considering this load will help in studying the load bearing capacity of the soil and ending up with results that are beneficial to terramechanics studies, so improvement in the machine design or choosing the suitable machine for specific terrain. This review shows the studies and models that researchers obtained and dealt with regarding the load bearing capacity. The techniques and the measurements used in finding the load bearing capacity of soil will be explained (Bevamer, Cone penetrometer).

**Keywords:** Load bearing capacity; Vehicle-terrain interaction; Bevamer; Cone penetrometer; Terrain; Soil pressure-sinkage; Terrain properties; Soil strength

### 1. Introduction

Off-road vehicles are used in many worldwide fields such as agricultural, construction, cross-country transportation, and also in military missions. Scientists have made heavy endeavours through the history in the fields of agriculture, logging, construction, mining, exploration, recreation, and military operations aiming to study locomotion over unprepared terrain.

Designing off-road vehicles and studying their interaction with the terrain have attracted many researcher's interests.

Studying the performance of an off-road vehicle on a terrain has become known as "Terramechanics". Terramechanics plays an important role in the development and evaluation of off-road equipments to be used on a specific terrain.

Over the years variety of methods of approach for studying off-road vehicles mobility have been developed including empirical methods, computational methods and methods for parametric analysis (Wong, 2010).

The forces and moments between the machine and the ground reflect the performance of the vehicle (Taheri, et al., 2015). So, the mobility of the vehicle and its dynamical performance are determined by the terrain-soil interaction during operation (Shibly & Iagnemma, 2005).

Terrain-vehicle machines provide guiding principles to understand better the soil-vehicle interaction. Most frequent problems faced during soil-machine interaction are encountered in the categories of excessive soil compaction, excessive wheel or track sinkage due to ground pressure, physical characteristics of both soil and vehicle, excessive wheel or tracks slippage and insufficient traction resulting from internal soil shear or surface friction failure (Yong et al., 1984).

Terrains mechanical properties are divided into two directions: the normal (load bearing capacity; pressure-sinkage relationship equations) and the tangential (shear load; shear-slippage relationship equations) (Bekker, 1969).

Normal load applied by the wheel on the terrain will compact the soil (reduction of soil pores volume), thus the wheel sinks until soil produces resistance load opposing the sinkage (is the load bearing capacity). The soil resistance to the wheel normal load is directly affected by the two soil parameters: cohesiveness (bonding of soil particles) and angle of internal friction (resistance of movement between soil particles), thus the soil resistance is influenced by the soil density, shear strength, and the load coming from the vehicle (Meirion-Griffith & Spenko, 2014).

Classifying the soil from its colour detected using a colour technique will help in determining the attributes of the (soil), so documenting differences between different soil types and their structures. Specifying the color of the soil would greatly help in avoiding overloading the soil beyond its capacity, so preventing soil compaction and other degradation factors.

The forces and moments acting at the interaction level are proportional to operating factors as slip ratio, slip angle, normal load, and tyre inflation pressure.

The pressure (stresses) at the contact part cause geometrical and mechanical changes in the tyre and the terrain as changing in the tyre belt deformation, soil sinkage, soil deformation, erosion, and particle's movement.

Mechanical changes in the tyre and the terrain occur upon interaction (bulk density, compaction, water content).

The deformable terrains in off-road scenarios increase the complexity of modelling the cases at the contact zone (Gallrein & Bäcker, 2007). For simplifying this interaction majority of terramechanics models make certain prior assumptions. These simplifications depend on the model's applicability and necessitates computational and experimental resources (Gipser, 2007).

## 2. The Structure and the Strength of the Soil

The soil is divided into two main types: cohesive and a frictional type; In general soils are combination of both friction and cohesive (Inns & Kilgour, 1978).

Cohesive forces depend on soil moisture suction rather than soil moisture content (Earl, 1996). Friction is the resistance between the soil particles when sliding over each other (Increase with the increase in the number of particles contacts per unit volume) (Dumbleton & West, 1970). The increase in soil bulk-density will increase the soil friction (Godwin et al., 1991).

Figure 1. shows the Mohr-Coulomb diagrams of the three soil classes are:

- a- Pure cohesive soil and possess only a cohesive (non-frictional) strength component; the water-saturated clay is an example of it.
- b- Pure frictional soil and has only frictional (zero cohesion) strength component; the dry sand is an example of this kind.
- c- Cohesive-frictional soil class and contains both cohesive and frictional strength components; the saturated clays, loams, and sands are examples of this soil class.

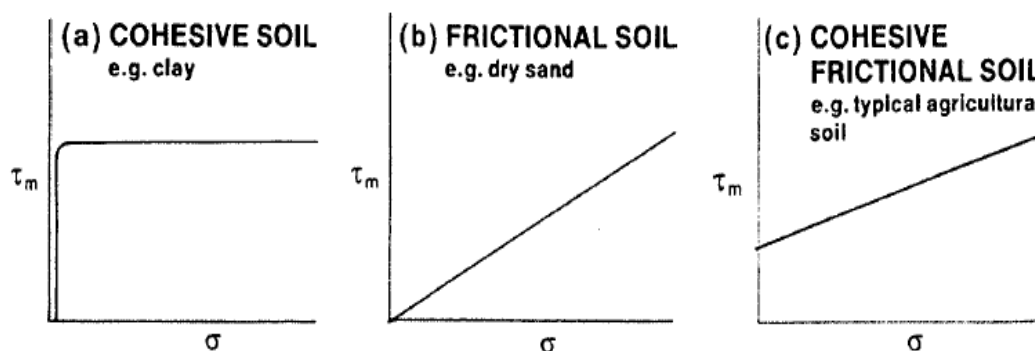


Figure 1. Graphs showing the strength of different soil types (Inns & Kilgour, 1978).

Freitag reported that it is important to consider the tractive performance on the three different soil classes (cohesive, frictional, cohesive-frictional) (Freitag, 1965).

### 2.1. Distribution of the Applied Load Stresses in the Terrain

The terrain under the vehicle is modelled as either elastic medium or as a rigid, perfectly plastic material (Wong, 2010). The elastic behaviour of a material is its tendency to return back to its original geometry, but when the material enters the plastic region then it is permanently deformed and will not return back to its initial geometry when removing the exerted load. The two regions are shown in the stress strain diagram shown in Figure 2.

The elasticity theory leads to the development of most theoretical investigations dealing with dense soil (for the limitation of need exceeding load bearing capacity the plastic theory reflect the soil failure) (Taghavifar & Mardani, 2017).

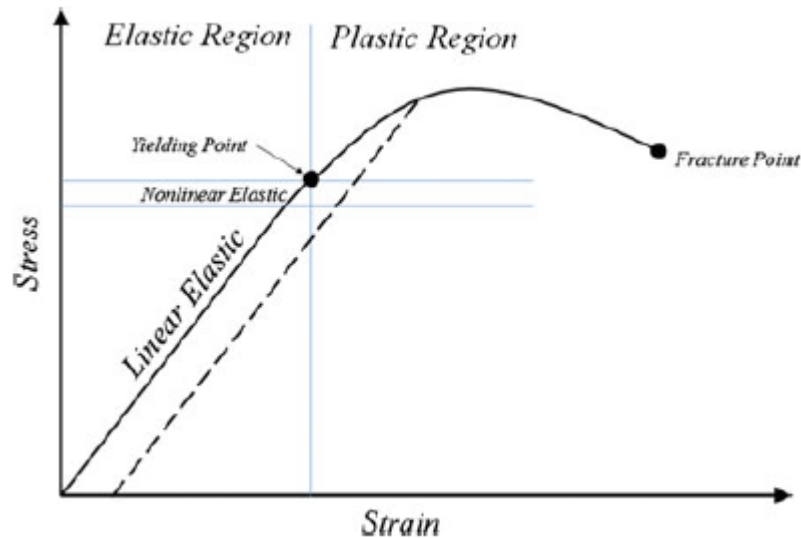


Figure 2. Soil Stress-Strain curve showing the elastic and plastic regions (Taghavifar & Mardani, 2017).

### 2.2. Moisture Content

The moisture is a component present in the soil structure, and that is based on the soil's three phase-system (minerals, moisture, and air). The moisture affects the characteristics of the soil such as consistency, compatibility, cracking, swelling, shrinkage, and the density.

Determining the water content in the soil is important in agriculture, mechanical, geotechnical, hydrological, and environmental engineering since moisture has impact on the soil's characteristics (Susha et al., 2014).

## 3. Load Bearing Capacity Measurement Techniques

Bevameter and cone penetrometer are two techniques that are used for measuring the terrain properties. Specifying which technique will be used depends on the type of vehicle used on the terrain, as an example for that the technique used in military vehicles is much different than the technique required by normal non-military vehicles. Selecting the suitable technique among both depends on the method of approaching the purpose. In case a technique is required by an off-road vehicle engineer in the development of new products, then the targeted technique is much different than the technique used for military vehicle trafficking on a go/no go basis (Wong, 2010).

### 3.1. Cone penetrometer Technique

This technique was initially used by the US army Engineer for evaluating the strength of soil (Freitag, 1966). In agricultural field the cone penetrometer is standardized as ASAE S313.2; by following the standard, the findings are compared to the standardized data (Figure 3.).

The index application range, penetration speed, and the depth increment for various penetrometer types are defined by the ASAE standard.

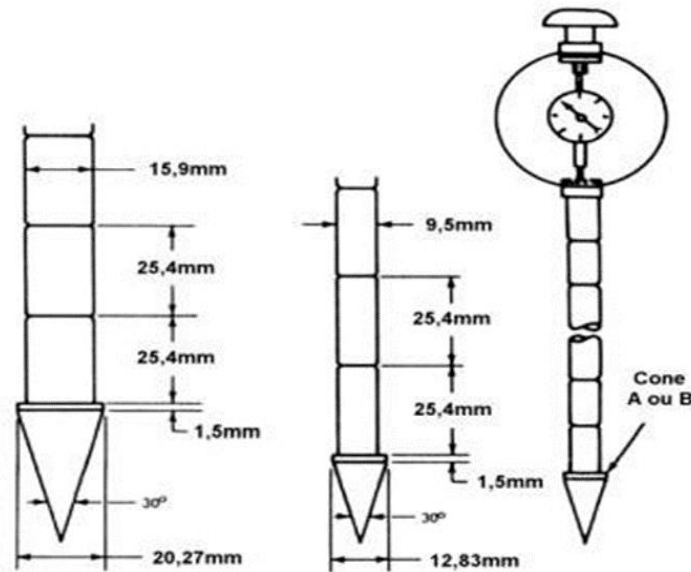


Figure 3. ASAE S313.2 Standardized cone penetrometer (Wong, 2010).

The value obtained from the cone penetrometer test is the cone index. This value indicates the average penetration force and is the force exerted by the soil against the conical head per unit projected cone base. The soil is penetrated by the cone to a given depth at a rate 3 cm/sec (suggested by ASAE). The value (cone index) is a composite value embedding the impact of shear, compression, and even soil metal friction (ASAE, 1988).

The CI (cone index) varies depending on the depth, so averaging of the CI values taken at different depths corresponding to the track or tyre sinkage will help in predicting the traction (Wismer & Luth, 1973).

The remoulding index (RI) is a value that measures the change in the terrain strength resulting from the passage of vehicles over terrains (recurrent activity). RI is the ratio of the soil's cone index after remoulding to that before remoulding (CI before). Regarding the remoulding test in case of fine-grained soils 100 blows of 1.135 kg (2.5 lb) hammer dropped from height 30.5 cm (12 in) on the soil sample in the remoulding cylinder, and in case of having coarse grained with fines soil type the hammer is dropped on the soil cylinder 25 times from 15.2 cm (6 in) height (SAE, 1967).

The RCI value-rating cone index-is the product of the remoulding index (RI) and the cone index (CI) before remoulding. The RCI shows the strength of terrain under repeated vehicle passage on it. In addition to this value there is the vehicle cone index, a value indicating trafficability and is the minimum soil CI at the critical layer level that allows the vehicle to move without getting immobilized. Considering the depth of the critical layer is dependent of the vehicle and its weight (Wong, 2010).

The cone index was calculated in term of terrain's angle of internal shearing resistance, cohesion, density, apparent shear modulus, and the cone shape and penetration depth (Rohani & Baladi, 1981).

An equation was developed by Hettiaratchi and Liang for the load acting on the cone or on a wedge-shape indenter. The equation was as function of the cone or wedge geometry, penetration depth, angle of internal shearing resistance, and terrain cohesion (Hettiaratchi & Liang, 1987).

The Cone index (CI), Remoulding index (RI), Rating cone index (RCI), Vehicle cone index (VCI), and slope index are values obtained by the penetrometer test (Taghavifar & Mardani, 2017).

The depth in the terrain influences the resulting CI value upon implementing the cone penetrometer test, so the CI value utilized for traction prediction is the average value of set of CI values recorded across different depths that correspond to maximum tyre or track sinkage (Wismar & Luth, 1973).

### 3.2. Bevameter Technique

This technique was developed by Bekker aiming to measure the strength of soil and its sinkage parameters upon being subjected to running wheel. The wheel or the running gear connected to the vehicle applies both the normal load (vertical) and the shear load (tangential stresses) on the terrain. The wheel contacts the terrain, thus transferring the power taken from the transmission to the wheels as tractive forces, so ending with the vehicle's movement.

For simulating the real wheel-terrain contact case through studying the normal and shear loads applied on the terrain, the Bevameter technique is the best among the others (Wong, 2010), (Wong, 2001).

The Bevameter technique (Figure 4.) embeds:

- The plate sinkage test; and it simulates the normal load applied from the running gear on the terrain, thus the pressure sinkage relationship of the soil.
- A shear test ending up with the In-situ shear strength parameters of the soil.

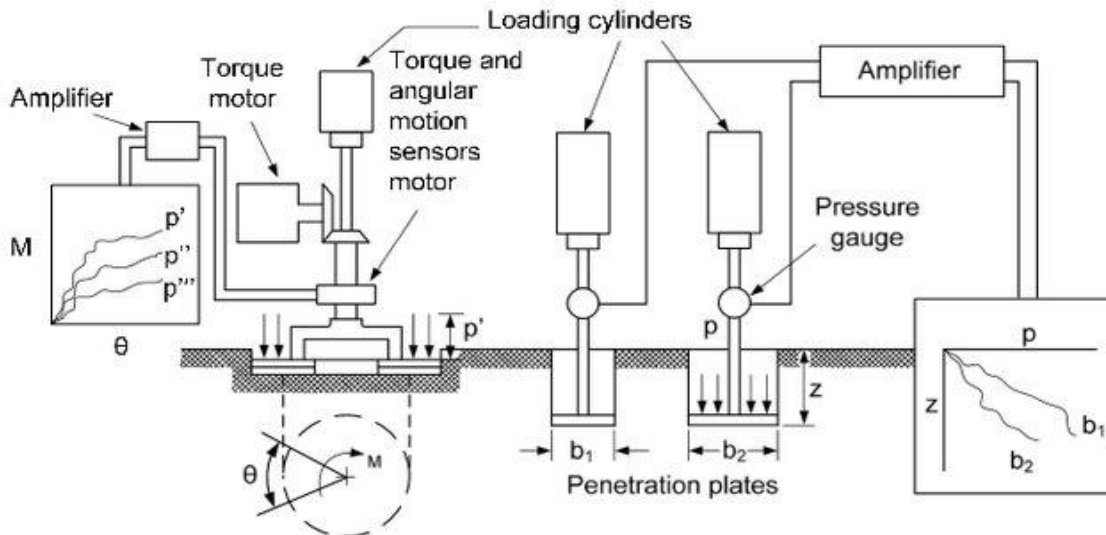


Figure 4. Bevameter schematic diagram (Bekker, 1969).

The shear device of the Bevameter holds an annular groused ring that is applied by a constant vertical load on the terrain, and when contacting the terrain, it is rotated at constant velocity. The torque and angular displacement are recorded for calculating the shear strength.

The normal load (in normal load test) is applied on the sand sample (terrain in reality) using different plates. Different sizes of flat plates are forced into the soil, and the penetration results are then recorded; reaching the load bearing capacity.

The Bevameter is associated with the following parameters: Cohesion (C), Angle of internal friction ( $\phi$ ), Sinkage moduli (k,  $k_c$ ,  $k_\phi$ ), Sinkage exponent (n) (Taghavifar & Mardani, 2017).

A custom built Bevameter at NASA Glenn research centre and is able to perform the two tests: the normal and the shear. For the normal test the instrument use a piston to press plate down (load cell measures the force, and a laser is measuring the vertical displacement) (Edwards et al., 2017).

When it comes to shearing the terrain (contact part), the same apparatus used in the normal test is also used for shearing having torque applied and the angular motion is measured by sensors (the resistance to rotation); simultaneously with the normal load applied.

#### 4. Studying the Normal Load Acting on the Terrain

Based on Boussinesq theory in elastic half-space, Saakyan (1965) suggested a pressure sinkage equation (Boussinesq, 1885; Nihal et al 2021).

$$p = k \left( \frac{Z}{D} \right)^n \quad (1)$$

where p is the average pressure under indenter, D is the diameter of the indenter, Z is the vertical soil deformation (sinkage), k is the sinkage modulus.

Bernstein in his field of expertise (agricultural engineering field) has demonstrated that if a plate penetrates soil (normal load) the pressure-sinkage curve arising is represented by the equation.

$$p \cong kz^{0.5} \quad (2)$$

where k is the modulus of inelastic deformation; 0.5 is the sinkage exponent (power); z is the depth (Bekker, 1969; Bernstein, 1913).

Later a Russian researcher adjusted the equation (2) by reducing it to the form.

$$p = kz^n \quad (3)$$

Considering the pressure-sinkage is of a power function form, then the above equation is an applicable equation, where k and n are curve fitting constants obtained experimentally for specific soil type with n ranging from 0 to 1 (represented in Figure 5)

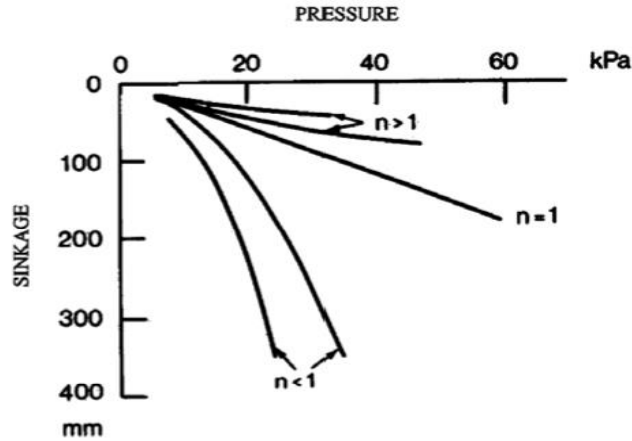


Figure 5. Typical pressure-sinkage curves (Bekker, 1969).

The limitations of this equation is that (k) and (n) are values of a particular soil type despite changing with surface load and the load range (Ageykin, 1973).

The plates used for performing the plate-sinkage experiment are either circular or rectangular considering that the width or the radius of plate influences the measured data (Bekker, 1956).

For homogeneous soil Bekker deduced that the above equation (3) can be reduced to the form:

$$p = \left( \frac{k_c}{b} + k_\phi \right) z^n \quad (4)$$

where b is the width used,  $k_c$  the pressure-sinkage parameter due to the cohesive effects,  $k_\phi$  the pressure-sinkage parameter due to the frictional effects, z is the sinkage of the plate, and  $n \in IR^*$  is the deformation exponent. (The  $k_\phi$  and  $k_c$  values are Independent of n value)

The equation above has shown its ability to measure the soil resistance to penetration over a wide soil range in addition to its ability in predicting trends when there isn't direct experimental data available (Wong, 2001).

In the above equation p and z are measured values, while  $k_c$ ,  $k_\phi$  and n are derived from the above equation (4).

Later Bekker modified equation 4 by introducing the weight of the vehicle:

$$z = \frac{3W}{\left( (3-n)(K_c + bK_\phi) d^2 \right)^{\frac{2}{2n+1}}} \quad (5)$$

where W is the wheel normal load, d is the tyre diameter, and b is the tyre width (Bekker, 1960).

Afterwards Onafeko and Reece mentioned that the pressure-sinkage relation depends on n.

Thus,

$$p = (c\hat{k}_c + \gamma b\hat{k}_\phi) \left( \frac{z}{b} \right)^n \quad (6)$$

where  $\hat{k}_c$ ,  $\hat{k}_\phi$ , and n are new dimensionless pressure-sinkage parameters, and  $\gamma$  is the specific weight of the terrain (Onafeko & Reece, 1967).

Wong proposed a weighted least squares method to obtain the parameters n,  $k_c$ ,  $k_\phi$ ,  $\hat{k}_c$  and  $\hat{k}_\phi$  (Wong, 2010). Thus, minimizing the function using a weighting Factor  $p^2$



$$F = \sum p^2 [\ln p - \ln k_{eq} - n \ln z]^2 \quad (7)$$

Where:  $k_{eq} = \frac{k_c}{b} + k_\phi$

Taking two partial derivatives of F (with respect to n and the other with respect to  $k_{eq}$ ) so, decreasing the values of F.

These two equations appear

$$\ln k_{eq} \sum p^2 \ln z + n \sum p^2 (\ln z)^2 = \sum p^2 \ln p \ln z \quad (8)$$

$$\ln k_{eq} \sum p^2 + n \sum p^2 \ln z = \sum p^2 \ln p \quad (9)$$

Since n depends on the size of the plate it is required to use an average n-value resulting from two different plates when calculating  $\ln k_{eq}$ . The usage of two different plates will result in two  $k_{eq}$  values (for  $b_1$  and  $b_2$  plates sizes).

The following equations can be used for determining  $k_c$  and  $k_\phi$ .

$$k_c = \frac{(k_{eq})_{b_1} - (k_{eq})_{b_2}}{b_2 - b_1} b_1 b_2 \quad (10)$$

$$k_\phi = (k_{eq})_{b_1} - \frac{(k_{eq})_{b_1} - (k_{eq})_{b_2}}{b_2 - b_1} b_2 \quad (11)$$

Wong defined the error between the experimental and theoretical data by developing a method known as “Goodness-of-fit” equation. This equation is the ratio of the mean square error to the mean value of pressure.

$$\varepsilon = 1 - \frac{\sqrt{\frac{\sum (p_m - p_{lc})^2}{N - 2}}}{\frac{\sum p_m}{N}} \quad (12)$$

where  $p_m$  is the measured pressure,  $p_{lc}$  is the calculated pressure (using above procedures), N is the number of data points used for the curve fitting  $\varepsilon = 1$  (perfect fit).

The increase in soil resistance is at greater depth since the pressure was not increasing the sinkage, and that results in a hyperbolic pressure-sinkage relation, and that is recognized in Figure 6, showing hyperbolic curves with the increase in the sinkage. Relying on semi-empirical methods for studying the soil behaviour under normal load would be better than extending the theory of elasticity and plasticity (Kougre et al., 1983).

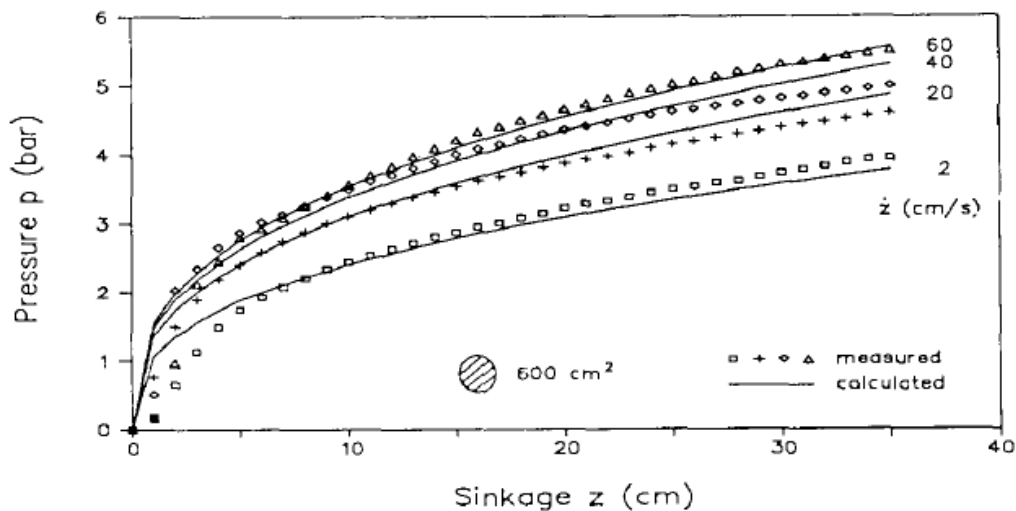


Figure 6. Measured and calculated pressure-sinkage curves (correlation) at different penetration velocities under 500 cm<sup>2</sup> loading surface (Grahn, 1991).

Emori and Schuring have shown that the force pushing the plate is function of the depth penetration ( $Z^*$ ), plate velocity ( $\dot{Z}$ ), and acceleration ( $\ddot{Z}$ ).

$$F_s = f_1(Z^*) + f_2(Z^*, \dot{Z}) + f_3(Z^*, \ddot{Z}) \quad (13)$$

$f_1$  is the static force,  $f_2$  is the force resulting from lateral acceleration of soil particle and viscosity,  $f_3$  is the inertial force vertically accelerated soil particles (Emori & Schuring, 1966).

The soil sinkage was smaller at higher penetration velocities and the modulus of soil deformation in Bekker's equation was equal to  $(K_0 \dot{Z}^m)$  where ( $\dot{Z}$ ) is the vertical velocity, ( $K_0$ ) is static modulus of soil deformation and ( $m$ ) is the exponent of soil penetration.

$$p = K_0 \dot{Z}^m Z^n \quad (14)$$

#### 4.1. Influence of the Plate Size and Shape

The plate penetration rate should always emulate the realistic case as in the track or wheel contact area. From a proof it is impossible to apply the load at high rate, because relating the load coming from a vehicle is not applied at high rate (major cases). Altering Bekker and Reece model resulting in equation (15).

$$p = (K_1 + 0.5bK_2)\beta^n Z^n \quad (15)$$

where  $\beta$  is a geometric constant (depends on plate shape). (Youssef & Ali, 1982).

Using plates that are of same sizes as the contact patch requires an increase in the plate's geometry with sinkage, also a new diameter would be required to be used in the equation. As a result of that Meirion-Griffith and Spenko worked on the effect of wheel diameter change on pressure sinkage.

Bekker model was modified to

$$p = \hat{K} z^{\hat{n}} D^{\hat{m}} \quad (16)$$

where  $D$  is the diameter,  $\hat{K}$  is the proposed sinkage modulus ( $\text{kN}/\text{m}^{\hat{n}+\hat{m}+2}$ ),  $\hat{n}$  is the proposed sinkage exponent,  $D$  is the wheel diameter, and  $\hat{m}$  is the diameter exponent. (Meirion-Griffith & Spenko, 2011).

The effect of the wheel width on sinkage was later used plus considering the effect of diameter.

$$z_0 = \frac{3W}{b(3 - \hat{n})\hat{k} \left( b\sqrt{Dz_0 - z_0^2} \right)^{m+0.5}} \quad (17)$$

$W$  is the normal load from the wheel and  $z_0$  is now a function of itself and cannot be separated. Such equation has no closed form solution. However, if every possible value of  $z_0$  inside the length function is plotted against the solution for  $z_0$  it can be seen that the two converge only once for sinkages less than the wheel radius, and yielding the correct solution (Meirion-Griffith & Spenko, 2013).

It is important to have proper and accurate prediction of the contact patch stresses, in addition to specifying the wheel load, tyre inflation pressure, recommended tyre inflation pressure, tyre width and diameter as input data to the soil compaction models increasing the accuracy of soil stress and compaction. (Keller, 2005).

Giving consideration to the pressure sinkage rate, Pope assumed that this relation fit as power law forming (Pope, 1969):

$$p = p_0 \left( \frac{u}{u_0} \right)^m \quad (18)$$

Using Reece model, the new equation is;

$$p = (ck_c + \gamma bk_\phi) \left( \frac{z}{b} \right)^n \left( \frac{u}{u_0} \right)^m \quad (19)$$

$u$  is the sinkage velocity,  $u_0$  is the plate sinkage;  $m$ ,  $n$  sinkage exponent.

It is important to note that an inclined load applied on a horizontal plate leads to more sinkage when compared to having the same load applied normally on the same plate. The sinkage of an inclined plate under an inclined load is less than the sinkage upon having vertical load applied on an inclined plate. (Xuewu et al, 1996).



### 5. Bevameter test at the University Laboratory

A bevameter test was carried out at the Hungarian University of Agriculture and Life Sciences laboratory. The bevameter used is shown in the Figure 7 and of a pressing plate diameter 20 cm. The load (normal load of increasing value) was applied using hydraulic force to press down the loam sand soil; loads were measured using a load cell and provided to the computer. Upon having the plate sinking the longitudinal deformation was also recorded using a displacement sensor and provided to the computer through the data logger. The results (load and displacement) recorded by the computer using the Catman 4.5 software, the results are shown in graphs plotted using excel as in Figure 8; of the soil at different moisture contents (0%, 10%, 20%).



Figure 7. Bevameter test at the university laboratory testing the loam sand soil at different moisture contents

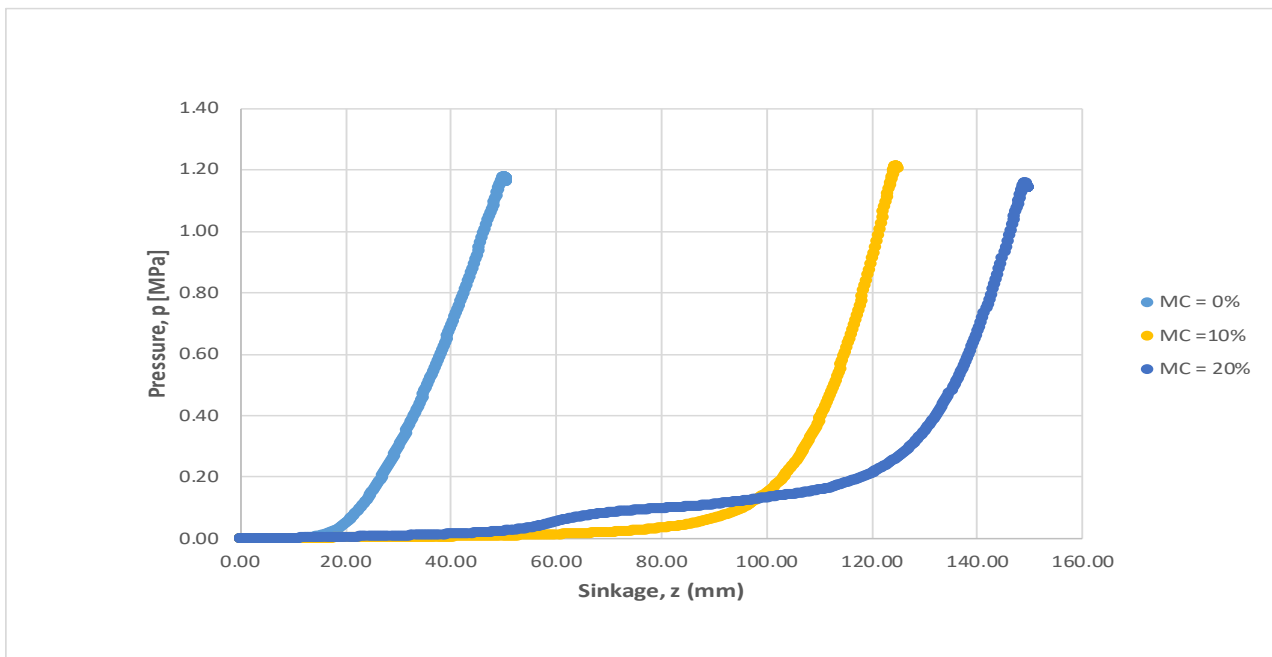


Figure 8. Pressure-sinkage curves at different moisture contents (0%, 10%, 20%) under plate size (D = 20 cm)

## 6. Numerical methods

The finite and discrete element methods are practical tools used for analysing complicated systems. These methods have been used in terramechanics modelling since 1970s and the popularity of using these methods continued to increase due to providing improved computational results (Wong, 2001).

Finite element method was used to study the potential self-excitation of wheeled-vehicles operating on soft soil. The discrete element method terramechanics is able to deal with complex effects arising during traversal through rough terrains by modelling the individual grain particles (Smith & Peng, 2013).

## 7. Conclusion

Many fields (agricultural, military...) require enhancements in the vehicles used and if not enhancing, choosing the suitable vehicle for the specified mission might be helpful in accomplishing it. The load bearing capacity will help in this enhancement by measuring the normal interaction between the vehicle and the terrain. The Bevameter and the cone penetrometer have facilitated measuring the resulting load bearing capacity between the vehicle and the terrain.

The cone penetrometer results with index value that is used for deducing many properties regarding the interaction, and the other technique (Bevameter) helps in measuring the normal displacement upon having normal load pressing on the terrain having at the same time the displacement being measured with the sinkage, so the resulting curve will help in studying the bearing capacity of the terrain.

Studying this normal load based on the equations and models proved by researchers, and by linking these models accurate study of the load bearing capacity as mentioned in the section (4) will be reached, in addition to considering the change in the wheel diameter, width, and tyre inflation on the load result and the geometry of the track in case of tracked vehicles.

Based on our experimental test made on loam sand soil, it has appeared that with the increase in the amount of moisture content present in the soil, the sinkage of the Bevameter plate increased upon applying the same load. So, we can deduce that the bearing capacity of the soil decreases with the increase in the moisture content. In reality this deduction is recognized when having a vehicle moving on wet soil (of the used type), that the increase in the amount of water in soil (wet soil) leads to the sinkage of the vehicle. We should also consider that on dry soil types (dry sand soil) the behaviour will be the opposite, where the increase in moisture content will increase the traction and the load bearing capacity of the soil.

Finally, even though using the Bevameter and the cone penetrometer techniques end up with beneficial results, in case of dealing with complicated cases (complicated interaction flow) numerical methods might be helpful in solving these cases by having these methods emulating the real interaction, such as using the finite element method or the discrete element method (studying the motion at the particle level).

## Acknowledgement

This work was accomplished by the help of the Mechanical Engineering Doctoral School at the Hungarian University of Agriculture and Life Sciences, Gödöllő, Hungary. Also, we would like to thank The Stipendium Hungaricum foundation for funding our Ph.D. program.

## References

- [1] **Ageykin, Y. S.** (1973). Evaluation of ground deformability with respect to vehicle mobility. *Journal of Terramechanics*, 10 (1), 105–111.
- [2] **Bekker, M.**, (1956). *Theory of Land Locomotion: The Mechanics of Vehicle Mobility*. University of Michigan Press, Ann Arbor, MI.
- [3] **Bekker, G.**, (1960). *Off-road Locomotion*. University of Michigan Press, Ann Arbor, MI.
- [4] **Bekker, M. G.** (1969). *Introduction to terrain-vehicle systems*. University of Michigan Press; First Edition edition (March 1, 1969).
- [5] **Bernstein, R.** (1913). Probleme zur experimentellen Motorpflugmechanik. *Der Motorwagen*, 16(9), 199–206.
- [6] **Boussinesq, J.**: Application des potentials a l'etude de l'equilibre et due mouvement des solides elastique, Gauthier-Villars, Paris, 1885. [Google Scholar](#).
- [7] **Dumbleton, M. J., & West, G.** (1970). the suction and strength of reiviloulded soils. Berkshire.

- [8] Earl, R. (1996). Prediction of Trafficability and Workability using Tensiometers. *Journal of Agricultural Engineering Research*, 63(1), 27–33. <https://doi.org/10.1006/jaer.1996.0004>.
- [9] Edwards, M. B., Dewoolkar, M. M., Huston, D. R., & Creager, C. (2017). Bevameter testing on simulant Fillite for planetary rover mobility applications. *Journal of Terramechanics*, 70, 13–26. <https://doi.org/10.1016/j.jterra.2016.10.004>.
- [10] Emori, R., & Schuring, D. (1966). static and dynamic penetration test of soil. *Journal of Terramechanics*, 3(1), 23–30.
- [11] Freitag D.R., (1965), Wheels on soft soils, an analysis of existing data. Technical Report No. 3-670 USAE Waterways Experiment Station.
- [12] Freitag, D. R. (1966). A dimensional analysis of the performance of pneumatics tires on clay. *Journal of Terramechanics*, 3(3), 51–68. [https://doi.org/10.1016/0022-4898\(66\)90106-6](https://doi.org/10.1016/0022-4898(66)90106-6).
- [13] Gallrein, A., & Bäcker, M. (2007). CD Tire: a tire model for comfort and durability applications. *Vehicle System Dynamics*, 45 (sup1), 69–77. <https://doi.org/10.1080/00423110801931771>.
- [14] Gipser, M. (2007). FTire – the tire simulation model for all applications related to vehicle dynamics. *Vehicle System Dynamics*, 45 (sup1), 139–151. <https://doi.org/10.1080/00423110801899960>.
- [15] Godwin, R. J., Warner, N. L., & Smith, D. L. O. (1991). The development of a dynamic drop-cone device for the assessment of soil strength and the effects of machinery traffic. *Journal of Agricultural Engineering Research*, 48(C), 123–131. [https://doi.org/10.1016/0021-8634\(91\)80009-4](https://doi.org/10.1016/0021-8634(91)80009-4).
- [16] Grahn, M. (1991). Prediction of sinkage and rolling resistance for off-the-road vehicles considering penetration velocity. *Journal of Terramechanics*, 28 (4), 339–347. [https://doi.org/10.1016/0022-4898\(91\)90015-X](https://doi.org/10.1016/0022-4898(91)90015-X).
- [17] Griffith, G. M., & Spenko, M. (2014). Simulation and experimental validation of a modified terramechanics model for small-wheeled vehicles. *International Journal of Vehicle Design*, 64(2/3/4), 153. doi:10.1504/ijvd.2014.058499.
- [18] Hettiaratchi, D. R. P., & Liang, Y. (1987). Nomograms for the estimation of soil strength from indentation tests. *Journal of Terramechanics*, 24 (3), 187–198. [https://doi.org/10.1016/0022-4898\(87\)90040-1](https://doi.org/10.1016/0022-4898(87)90040-1).
- [19] Inns, F. M., & Kilgour, J. (1978). *Agricultural tyres*. London: Dunlop. Retrieved from [http://books.google.co.uk/books/about/Agricultural\\_tyres.html?id=JB8NAQAAMAAJ&pgis=1](http://books.google.co.uk/books/about/Agricultural_tyres.html?id=JB8NAQAAMAAJ&pgis=1).
- [20] Keller, T. (2005). A Model for the prediction of the contact area and the distribution of vertical stress below agricultural tyres from readily available tyre parameters. *Biosystems Engineering*, 92 (1), 85–96. <https://doi.org/10.1016/j.biosystemseng.2005.05.012>.
- [21] Kogure, K., Ohira, Y., & Yamaguchi, H. (1983). Prediction of sinkage and motion resistance of a tracked vehicle using plate penetration test. *Journal of Terramechanics*, 20 (3–4), 121–128. [https://doi.org/10.1016/0022-4898\(83\)90043-5](https://doi.org/10.1016/0022-4898(83)90043-5).
- [22] Meirion-Griffith, G., & Spenko, M. (2011). A modified pressure-sinkage model for small, rigid wheels on deformable terrains. *Journal of Terramechanics*, 48 (2), 149–155. <https://doi.org/10.1016/j.jterra.2011.01.001>.
- [23] Meirion-Griffith, G., & Spenko, M. (2013). A pressure-sinkage model for small-diameter wheels on compactive, deformable terrain. *Journal of Terramechanics*, 50 (1), 37–44. <https://doi.org/10.1016/j.jterra.2012.05.003>.
- [24] Onafeko, O., & Reece, A. R. (1967). Soil stress and deformation beneath rigid wheels. *Journal of Terramechanics*, 59 (1), 59–80.
- [25] Pope, R. G. (1969). The effect of sinkage rate on pressure sinkage relationships and rolling resistance in real and artificial clays. *Journal of Terramechanics*, 6 (4), 31–38. [https://doi.org/10.1016/0022-4898\(69\)90015-9](https://doi.org/10.1016/0022-4898(69)90015-9).
- [26] Rohani, B., & Baladi, G. Y. (1981). Correlation of mobility cone index with fundamental engineering properties of soil. U. S. Army Grgnee Watewy xprmn Station. Vicksburg.
- [27] SAE. (1967). *Off-road Vehicle Mobility Evaluation*. S.A.E.
- [28] Salman, N.D.; Pillinger, G.; Hanon, M.M.; Kiss, P. (2021) A Modified Pressure–Sinkage Model for Studying the Effect of a Hard Layer in Sandy Loam Soil. *Appl. Sci.* 2021,11, 5499. <https://doi.org/10.3390/app11125499>.

- [29] Shibly, H., & Iagnemma, K. (2005). An equivalent soil mechanics formulation for rigid wheels in deformable terrain , with application to planetary exploration rovers, 42, 1–13. <https://doi.org/10.1016/j.jterra.2004.05.002>.
- [30] Smith, W., & Peng, H. (2013). Modeling of wheel-soil interaction over rough terrain using the discrete element method. Journal of Terramechanics, 50 (5–6), 277–287. <https://doi.org/10.1016/j.jterra.2013.09.002>.
- [31] Susha Lekshmi S.U., D.N. Singh, Maryam Shojaei Baghini, (2014) A critical review of soil moisture measurement, Measurement, Volume 54, 2014, Pages 92-105, <https://doi.org/10.1016/j.measurement.2014.04.007>.
- [32] Saakyan, S. (1965) ‘Soil resistance under load’, Szbornyik trudov po zeml, Vol. 3, pp.24–31.
- [33] Taghavifar, H., & Mardani, A. (2017). Off-road Vehicle Dynamics (Vol. 70). Switzerland: Springer International Publishing. <https://doi.org/10.1007/978-3-319-42520-7>.
- [34] Taheri, S., Sandu, C., & Taheri, S. (2014). Finite Element Modeling of Tire Transient Characteristics in Dynamic Maneuvers. SAE International Journal of Passenger Cars - Mechanical Systems, 7 (1), 2014-01–0858. <https://doi.org/10.4271/2014-01-0858>.
- [35] Wismer, R. D., & Luth, H. J. (1973). Off-road traction prediction for wheeled vehicles. Journal of Terramechanics, 10 (2), 49–61. [https://doi.org/10.1016/0022-4898\(73\)90014-1](https://doi.org/10.1016/0022-4898(73)90014-1).
- [36] Wong, J. Y. (2001). Theory of Ground Vehicles (Third). Canada: JOHN WILY and SONS.
- [37] Wong, J. Y. (2010). Terramechanics and Off-Road Vehicle Engineering (Second). Oxford, UK: Elsevier Ltd. <https://doi.org/10.1016/C2009-0-00403-6>.
- [38] Xuewu, J., Jide, Z., & Xiding, Q. (1996). Effects of loading patterns on the pressure-sinkage relation of dry loose sand. Journal of Terramechanics, 33 (1), 13–20. [https://doi.org/10.1016/0022-4898\(96\)00005-5](https://doi.org/10.1016/0022-4898(96)00005-5).
- [39] Yong, R. N., Fattah, E. A., & Skiadas, N. (1984). Vehicle Traction Mechanics. Amsterdam: Elsevier Science.
- [40] Youssef, A.-F. A., & Ali, G. A. (1982). Determination of Soil Parameters using Plate Test. Journal of Terramechanics, 19 (2), 129–147. [https://doi.org/10.1016/0022-4898\(82\)90016-7](https://doi.org/10.1016/0022-4898(82)90016-7).